



RESEARCH ARTICLE

STUDY OF IDENTIFICATION OF CRIMINALS AND DUPE BY ANDROGENIC HAIR PATTERNS

Praveen R. Joshi

Electronics Terna Engineering College, Nerul, Navi Mumbai

ARTICLE INFO

Article History:

Received 19th, September, 2015

Received in revised form 27th, September, 2015

Accepted 13th, October, 2015

Published online 28th, October, 2015

Key words:

Androgenic hair pattern, biometric trait, low-resolution.

ABSTRACT

Identifying criminals and victims is always an important task in police investigation and forensic evaluation. Finger marks, blood samples, DNA, dental records, tattoos, face images and face sketches are used regularly by law enforcement agents all around the world. However, they cannot handle the cases, where only images describing crime scene specimens are available. Nowadays Identifying criminals and victims in images (e.g., child pornography and masked gunmen) can be a challenging task, especially when neither their faces nor any mark are observable. Skin mark patterns and blood vessel patterns are recently proposed to address this problem. However, they are invisible in low-resolution images and dense androgenic hair can cover them completely. Medical research results have implied that androgenic hair patterns are a stable biometric trait and have potential to overcome the weaknesses of skin mark patterns and blood vessel patterns. We are using Artificial Neural Network for the matching of the images. It is a fast growing field. To the best of our knowledge, no one has studied androgenic hair patterns for criminal and victim identification before. This paper aims to study matching performance of androgenic hair patterns in low resolution images.

© Copy Right, Research Alert, 2015, Academic Journals. All rights reserved.

INTRODUCTION

Criminals and victims in images describing crime-scene specimen identifying is a challenging task, especially when neither faces nor tattoos are observable. Though blood vessel patterns and skin mark patterns have been proposed to address this problem, they demand high resolution images to visualize hidden blood vessels and accurately detect skin marks. Though hairs collected in crime scenes are regularly used for forensic analysis, according to our best knowledge, androgenic hair patterns in images were never studied for criminal and victim identification. For matching androgenic hair patterns, we propose an algorithm based on a dynamic grid system and Gabor orientation histograms.

Androgenic hair patterns in low resolution images are an effective biometric trait and the proposed Gabor orientation histograms are comparable with other well-known texture recognition methods, including local binary patterns, local Gabor binary patterns and histograms of oriented gradients. This paper exposes a new way to address the challenging criminal and victim identification problem. In forensic identification, image quality is always a problem. Images of child pornography, masked gunmen and violent protestors are our targets.

Child pornographic images often have good quality because pedophiles enjoy high quality images. For cases of masked gunmen and violent protestors, the original images can be taken by reporters, who always use professional DSLR cameras, e.g. Canon EOS 10DX. Sometimes good quality images are obtained. For web images describing crime-scene specimen, no matter what cameras are used to take the original images, one great challenge is low resolution, which is the focus of this paper. Although the resolution of surveillance videos is also very low, the challenges in surveillance images and web images are different. Surveillance cameras are always mounted in high positions. They likely capture head-print, instead of androgenic hair.

Androgenic hair patterns in low resolution images can be used as a biometric trait for criminal and victim identification. However, low resolution is only one of the problems. For robust identification, new algorithms should be developed for viewpoint and pose variations and occlusions. These algorithms can enhance the performance of the proposed algorithm, which uses the dynamic grid system and the features to absorb all variations and distortions. In addition, an automatic segmentation algorithm should be developed to reduce manpower, even though a semi-automatic approach is not uncommon in forensic analysis. Once law enforcement agents use androgenic hair patterns in real applications, numerous images can be collected from

inmates and suspects for this research direction. Though low resolution images are the focus of this paper, androgenic hairs and their follicles in high resolution images should also be studied, because in child pornography cases, high resolution and close up images are commonly obtained. In addition to searching a suspect in a given database, how to assign evidential values in the form of a likelihood ratio to androgenic hair patterns is also equally important.

The Proposed Androgenic Hair Pattern Identification Algorithm

The proposed androgenic hair pattern identification algorithm has three computational components, preprocessing, feature extraction and matching. The algorithm takes a color leg image as an input and compares it with templates in a given database. First, the input leg image is segmented and normalized. The segmentation process is to remove all irrelevant information e.g. background. The normalization process is to identify the common region and standardize the image size for matching. Real parts of Gabor filters with different scales and orientations are then applied to the preprocessed image to compute Gabor magnitudes. These magnitudes are combined to extract local orientations and form an orientation field. It is divided into small regions for computing local orientation histograms as features. Finally, these histograms are matched with those in the database.

Preprocessing

Gray scale conversion

It is also known as an intensity, gray scale, or gray level image. Array of class uint8, uint16, int16, single, or double whose pixel values specify intensity values. For single or double arrays, values range from [0, 1]. For uint8, values range from [0,255]. For uint16, values range from [0, 65535]. For int16, values range from [-32768, 32767]. It is also known as an RGB image.

A true color image is an image in which each pixel is specified by three values one each for the red, blue, and green components of the pixel scalar. M by-n-by-3 array of class uint8, uint16, single, or double whose pixel values specify intensity values. For single or double arrays, values range from [0,1]. For uint8, values range from [0, 255]. For uint16, values range from [0, 65535].

In RGB color model, each color appears in its primary spectral components of red, green and blue. The color of a pixel is made up of three components; red, green, and blue(RGB), described by their corresponding intensities. Color component are also known as color channels or color planes (components). In the RGB color model, a color image can be represented by the intensity function.

$$I_{RGB} = (F_R, F_G, F_B)$$

Where $F_R(x,y)$ is the intensity of the pixel (x,y) in the red channel, $f_G(x,y)$ is the intensity of pixel (x,y) in the Green-channel, and $f_B(x,y)$ is the intensity of pixel (x,y) in the blue channel. The intensity of each color channel is usually stored

using eight bits, which indicates that the quantization level is 256. That is, a pixel in a color image requires a total storage of 24 bits.

Original image



Fig.1 Original Image

Gray scale converted image



Fig2 Gray Scale Image

A 24 bit memory can express as

$$224 = 256 \times 256 \times 256 = 16777216$$

If only the brightness information is needed, color images can be transformed to gray scale images [4]. The transformation can be made by using proposed equation.

$$I_y = 0.333F_r + 0.5F_g + 0.1666F_b$$

Where F_r , F_g and F_b are the intensity of R, G and B component respectively and I_y is the intensity of equivalent gray level image of RGB image. In RGB pixel information image there are three component (R,G,B) When RGB image converted into gray image then the intensity of pixel (1, 1) can be calculated by using the pixel values of RGB image in above transformation.

Median Filter

Noise may be introduced into an image in a number of different ways. In the previous section we talked about how to remove noise that has been introduced in an additive fashion. Here we look at a different noise model, one where a small number of pixels are corrupted due to, for example, a faulty transmission line. The corrupted pixels randomly take on a value of white or black, hence the name salt and pepper used to describe such noise patterns. The disastrous result of

applying the solution from the additive noise model (Wiener filter) to the salt and pepper noise image in the top panel. Trying to average out the noise in this fashion is equivalent to asking for the average salary of a group of eight graduate students and Bill Gates. As the income of Gates will skew the average salary so does each noise pixel when its value is so disparate from its neighbors. In such cases, the mean is best replaced with the median, computed by sorting the set of numbers and reporting on the value that lies midway. The much improved result of applying a 3×3 median filter to the salt and pepper noise image.

More specifically, the center pixel of each 3×3 neighborhood is replaced with the median of the nine pixel values in that neighborhood. Figure 8.2 15×15 median filter Depending on the density of the noise the median filter may need to be computed over a larger neighborhood. The tradeoff being that a larger neighborhood leads to a loss of detail, however this loss of detail is quite distinct from that of averaging. For example, shown in Notice that although many of the internal details have been lost the boundary contours (edges) have been retained, this is often referred to as posterization. This effect could never be achieved with an averaging filter which would indiscriminately smooth over all image structures. Because of the non-linear sorting step of a median filter it cannot be implemented via a simple convolution and is thus often more costly to implement. Outside the scope of this presentation there are a number of tricks for reducing the computational demands of a median filter.

Median Filtered Image



Fig3 Median filtered image

Edge Detection

Edge detection refers to the process of identifying and locating sharp discontinuities in an image. The discontinuities are abrupt changes in pixel intensity which characterize boundaries of objects in a scene. Classical methods of edge detection involve convolving the image with an operator (a 2-D filter), which is constructed to be sensitive to large gradients in the image while returning values of zero in uniform regions. There are an extremely large number of edge detection operators available, each designed to be sensitive to certain types of edges. Variables involved in the selection of an edge detection operator include Edge orientation, Noise environment and Edge structure. The geometry of the operator determines a characteristic direction in which it is most sensitive to edges. Operators can be optimized to look for horizontal, vertical, or diagonal edges. Edge detection is difficult in noisy images, since both the noise and the edges contain high frequency content.

Attempts to reduce the noise result in blurred and distorted edges. Operators used on noisy images are typically larger in scope, so they can average enough data to discount localized noisy pixels. results in less accurate localization of the detected edges. Not all edges involve a step change in intensity. Effects such as refraction or poor focus can result in objects with boundaries defined by a gradual change in intensity. The operator needs to be chosen to be responsive to such a gradual change in those cases. So, there are problems of false edge detection, missing true edges, edge localization, high computational time and problems due to noise etc. Therefore, the objective is to do the comparison of various edge detection techniques and analyze the performance of the various techniques in different conditions. There are many ways to perform edge detection.

However, the majority of different methods may be grouped into two categories:

Gradient based Edge Detection

The gradient method detects the edges by looking for the maximum and minimum in the first derivative of the image.

Laplacian based Edge Detection

The Laplacian method searches for zero crossings in the second derivative of the image to find edges. An edge has the one-dimensional shape of a ramp and calculating the derivative of the image can highlight its location.

Sobel Operator

The operator consists of a pair of 3×3 convolution kernels as shown in Figure 1. One kernel is simply the other rotated by 90° .

$$\begin{array}{|c|c|c|} \hline -1 & 0 & +1 \\ \hline -2 & 0 & +2 \\ \hline -1 & 0 & +1 \\ \hline \end{array} \quad G_x \qquad \begin{array}{|c|c|c|} \hline +1 & +2 & +1 \\ \hline 0 & 0 & 0 \\ \hline -1 & -2 & -1 \\ \hline \end{array} \quad G_y$$

These kernels are designed to respond maximally to edges running vertically and horizontally relative to the pixel grid, one kernel for each of the two perpendicular orientations. The kernels can be applied separately to the input image, to produce separate measurements of the gradient component in each orientation (call these G_x and G_y). These can then be combined together to find the absolute magnitude of the gradient at each point and the orientation of that gradient.

Edge Detected Image



Fig4 Edge detected image

Skin Pixel Segmentation

Hue-saturation based colorspace were introduced when there was a need for the user to specify color properties numerically. They describe color with intuitive values, based on the artist's idea of tint, saturation and tone. *Hue* defines the dominant color (such as red, green, purple and yellow) of an area, *saturation* measures the colorfulness of an area in proportion to its brightness. The "intensity", "lightness" or "value" is related to the color luminance. The intuitiveness of the color space components and explicit discrimination between luminance and chrominance properties made these colorspace popular in the works on skin color segmentation. Several interesting properties of Hue were noted in it is invariant to highlights at white light sources, and also, for matte surfaces, to ambient light and surface orientation relative to the light source. However, points out several undesirable features of these colorspace, including hue discontinuities and the computation of "brightness" (lightness, value), which conflicts badly with the properties of color vision.

$$H = \arccos \frac{\frac{1}{2}((R-G) + (R-B))}{\sqrt{((R-G)^2 + (R-B)(G-B))}}$$

$$S = 1 - \frac{\min(R, G, B)}{R + G + B}$$

$$V = \frac{1}{3}(R + G + B)$$

An alternative way of hue and saturation computation using log opponent values was introduced in where additional logarithmic transformation of RGB values aimed to reduce the dependence of chrominance on the illumination level. The polar coordinate system of Hue- Saturation spaces, resulting in cyclic nature of the color space makes it inconvenient for parametric skin color models that need tight cluster of skin colors for best performance.

Skin Detected Image



Fig5 Skin Detected Area

The grid oriented image is filtered with the Gabor filter to extract the features of the image like phase, frequency and orientation. The featured image is decompose with DWT decomposition to get the important image values in lower frequencies. Then the histogram of the particular image is calculated to find the variation of pixels in the image.

Grid Oriented Image

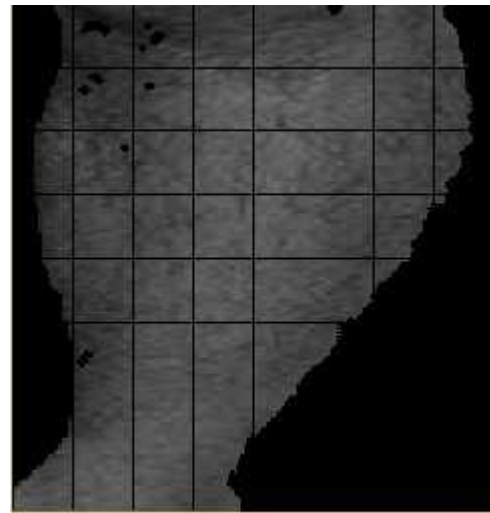


Fig 6 Grid oriented image

Future Work

The ANN (Artificial Neural Network) is used for the matching of the images. This document provides definitions and some results for tests that detect the presence of a condition (a test result is either "positive" or "negative", which may be "true" or "false").

Definition 1 -A true positive test result is one that detects the condition when the condition is present.

Definition 2 -A true negative test result is one that does not detect the condition when the condition is absent.

Definition -A false positive test result is one that detects the condition when the condition is absent. Definition 4 -A false negative test result is one that does not detect the condition when the condition is present.

Definition 5 Sensitivity measures the ability of a test to detect the condition when the condition is present. Thus, Sensitivity = TP/(TP+FN).

Definition 6-.Specificity measures the ability of a test to correctly exclude the condition (not detect the condition) when the condition is absent. Thus, Specificity = TN/(TN+FP).

Definition 7- Predictive value positive is the proportion of positives that correspond to the presence of the condition. Thus, Predictive value positive = TP/(TP+FP).

Definition 8- Predictive value negative is the proportion of negatives that correspond to the absence of the condition. Thus, Predictive value negative = TN/(TN+FN).

Definition 9- A parallel combination of tests is a test that is positive if at least one of the combining tests is positive; otherwise it is negative (alternative definition: a parallel combination of tests is a test that is negative only if all the combining tests are negative otherwise it is positive).

Definition 10- A series combination of tests is a test that is

negative if at least one of the combining tests is negative; otherwise it is positive (alternative definition: a series combination of tests is a test that is positive only if all the combining tests are positive; otherwise it is negative).

Two (or more) tests are independent if the result of any of the tests does not depend on the result of the other test(s).

Result 1- The sensitivity (SEN) and specificity (SPE) of a parallel combination of N independent. $SEN = 1 - (1 - SEN_1) \cdot (1 - SEN_2) \cdot \dots \cdot (1 - SEN_n)$ $SPE = SPE_1 \cdot SPE_2 \cdot \dots \cdot SPE_n$

Respectively, where i SEN is the sensitivity and i SPE the specificity of the i th combining test. Thus, a parallel combination of tests increases the sensitivity and decreases the specificity.

Result 2- The sensitivity (SEN) and specificity (SPE) of a series combination of N independent tests are $SEN = SEN_1 \cdot SEN_2 \cdot \dots \cdot SEN_n$ $SPE = 1 - (1 - SPE_1) \cdot (1 - SPE_2) \cdot \dots \cdot (1 - SPE_n)$

Respectively, where i SEN is the sensitivity and i SPE the specificity of the i th Combining test.

References

1. Ieee transactions on information forensics and security, vol. 9, no. 4, april 2014
2. K. S. Stenn and R. Paus, "Controls of hair follicle cycling," *Physiol. Rev.*, vol. 81, no. 1, pp. 449–491, 2001.
3. R. E. Billingham, "A reconsideration of phenomenon of hair neogenesis with particular reference to the healing of cutaneous wounds in adult mammals," in

- The Biology of Hair Growth, W. Montagna and R. A. Ellis, Eds. New York, NY, USA: Academic, 1958
4. A. Vogt, K. J. McElwee, and U. Blume-Peytavi, "Biology of the hair follicle," in *Hair Growth and Disorders*, U. Blume-Peytavi, Tosti, D. A. Whiting, and R. M. Trüeb, Eds. New York, NY, USA: Springer-Verlag, 2008.
5. H. B. Chase, "Growth of hair," *Phys. Rev.*, vol. 34, no. 1, pp. 113–126,
6. V. A. Randall and N. V. Botchkareva, "The biology of hair growth," in *Cosmetic Applications of Laser and Light-Based System*, G. S. Ahluwalia, Ed. Norwich, NY, USA: William Andrew Inc., 2009.
7. V. A. Randall and E. J. G. Ebling, "Seasonal changes in human hair growth," *Brit. J. Dermatol.*, vol. 124, no. 2, pp. 146–151, 1991.
8. Yusur Al-Nuaimi^{1,2}, Gerold Baier¹, Rachel E. B. Watson², Cheng-Ming Chuong³ and Ralf
9. BBC News. London, U.K. (2001, Mar. 26). International Child Porn Ring Smashed [Online]. Available: <http://news.bbc.co.uk/1/hi/world/amerIcas/1244457.stm>
10. [10] (2013). Canada's National Tipline for Reporting the Online Sexual Exploitation of Children [Online]. Available: http://www.cybertip.ca/pdfs/fact_sheet_pdfs/English/CyberStats_en.pdf
11. S. Bukhari, "Dress," Translation of Sahih Bukhari, vol. 7, book 72, no. 815, Center for Muslim–Jewish Engagement. Los Angeles, CA, USA, 2002
12. N. Dalal and B. Triggs, "Histograms of oriented gradients for human detection," in *Proc. CVPR*, 2005, pp. 886–893.
13. J. G. Daugman, "High confidence visual recognition of persons by a test of statistical independence," *IEEE Trans. Pattern Anal. Mach. Intell.*, vol. 15, no. 11, pp. 1148–1161, Nov. 1993
